

LLM Web Dynamics: Tracing Model Collapse in a Network of LLMs

Tianyu Wang[†]
Johns Hopkins University

Lingyou Pang
University of California, Davis

Akira Horiguchi
University of California, Davis

Carey E. Priebe
Johns Hopkins University

Abstract

The increasing use of synthetic data from the public Internet has enhanced data usage efficiency in large language model (LLM) training. However, the potential threat of model collapse remains insufficiently explored. Existing studies primarily examine model collapse in a single model setting or rely solely on statistical surrogates. In this work, we introduce LLM Web Dynamics (LWD), an efficient framework for investigating model collapse at the network level. By simulating the Internet with a retrieval-augmented generation (RAG) database, we analyze the convergence pattern of model outputs. Furthermore, we provide theoretical guarantees for this convergence by drawing an analogy to interacting Gaussian Mixture Models.

1 Introduction

Synthetic data is crucial for training and scaling large language models. On the one hand, neural-scaling law assumes model performance will improve as the amount of training data increases (Kaplan et al., 2020); on the other hand, the pool of human-generated data is approaching its natural limit (Villalobos et al., 2024). Augmenting the training data with synthetic text has therefore become a common remedy (Man and Chahl, 2022). However, recent evidence suggested that the usage of synthetic data can lead to issues including parameter degradation (Dohmatob et al., 2024), amplified biases (Wyllie et al., 2024), and, in the most extreme cases, model collapse: a process characterized by the loss of information about the raw data distribution when an LLM is iteratively trained primarily on its own previous outputs (Shumailov et al., 2024). Analyzing the process of model collapse, and more generally the perturbations from

synthetic data, is therefore essential for LLM training.

In our work, we introduce the *LLM Web Dynamics* (LWD)—a framework that renders the full life-cycle of synthetic data *tractable*, *measurable*, and *theoretically valid*. Our contributions are threefold:

1. Network-level model-collapse metric. We design a network of interacting LLMs in which pretrained models from API communicate, receive opinions from each other, and update memory via retrieval-augmented generation (RAG). Individual responses are mapped into an embedding vector space and then converted to a pairwise distance matrix which quantitatively captures response similarities. As collapse unfolds and response similarity rises, this matrix shows drifting in geometry features accordingly, which provides a model-agnostic stability measuring metric. This metric reflects the stabilization of collective communicating dynamics of all participant LLMs.

2. Internet ecosystem simulator (API-only, cost-efficient). We anticipate a near-future feedback loop where synthetic texts generated by LLM agents populate the Internet and are later reused as training data or prompt augmentations in downstream applications (Martínez et al., 2023; Seddik et al., 2024). Our LWD framework constructs a virtual reality that mirrors real-world, AI-rich Internet environment by deploying a centralized RAG memory updating algorithm. Since each agent operates solely through API-accessible models, the framework approximates incremental fine-tuning without the need for retraining or additional fine-tuning, while also enabling the exploration of more complex scenarios.

3. Theoretical grounding via a Gaussian Mixture Model (GMM) proxy. To validate the collapse process of our LLM system analytically, we construct an analogue network of GMMs. For a fixed prompt, an LLM’s answers form a probability distribution, and GMMs serve as density approxi-

[†] corresponding author: twang147@jhu.edu.

mators (Goodfellow et al., 2016). This proxy offers theoretical guarantees for our claims and serves as a cost-efficient tool for gaining preliminary insights into LLM behavior at larger scales.

2 Related Work

This phenomenon of model degradation is well documented and has been observed across domains, tasks, and model types. Alemohammad et al. (2023) introduce self-consuming training loops and show that, without a constant infusion of fresh real data, models converge to “Model Autophagy Disorder” (MAD). In image generation, Bohacek and Farid (2025) demonstrate that even a small share of self-generated images used during retraining triggers self-poisoning, reducing both realism and diversity. Shumailov et al. (2024) first formalize this phenomenon as model collapse and demonstrates its existence in practice via GMMs, variational autoencoders (VAEs), and LLMs.

Quantifiable and interpretable model collapse have also attracted many attention in recent literature. Statistical surrogates are commonly used to provide instrumentally similar insights into this problem. In particular, regression-based methods are applied to simulate the iterative training of LLMs because they yield closed-form analytical risk expressions (Dohmatob et al., 2024; Gerstgrasser et al., 2024; Kazdan et al., 2025). Surrogates with stronger distribution assumptions including Gaussian distributions, Gaussian processes, and GMMs provide a theoretically interpretable and tightly controllable testbed whose generative nature closely mirrors that of LLMs (He et al., 2025; Suresh et al., 2024; Borji, 2024; Li et al., 2024; Alemohammad et al., 2023).

A crucial finding is that collapse dynamics shall be decisively influenced by the strategy for accumulating and infusing synthetic data across training iterations. A full replace paradigm (Schaeffer et al., 2025; Dey and Donoho, 2024) refers to entire updating in training data. Gerstgrasser et al. (2024) and Kazdan et al. (2025) validate that the accumulation of synthetic data from all previous iterations effectively prevents the collapse of the model. Bertrand et al. (2024) only keeps the most recent batch of synthetic data and points out synthetic to real data ratio shows a more significant role in model collapse.

Recent work centers on establishing connection between model collapse and a varying synthetic-

to-real ratio. Gillman et al. (2024) reports that a moderate level of synthetic input helps preserve low-density diversity. He et al. (2025) prove that, for both mean and covariance estimation, the estimation error is minimized when the weight on real data equals the reciprocal of the golden ratio. Conversely, Dohmatob et al. (2024) show that collapse can arise even at very small amount of synthetic data, implying that the synthetic-to-real ratio must asymptotically approach zero to maintain model diversity. Similarly, Bertrand et al. (2024) argue that keeping the ratio below a certain threshold also promotes long-run stability of training.

These results highlight the *controllability* of model collapse. A systematic strategy for synthetic and real data combination shall lead to a framework of interpretable model uncertainty control, more efficient use of synthetic data, and, cheaper but safer scaling of LLMs. Despite these promises, current research still faces challenges. **(i) Disconnect from realistic web dynamics and synthetic data generation.** Most existing analyses rely on purely statistical models, not tailored to mimic real-world Internet ecosystems. Additionally, their experimental setups often involve collecting and recycling synthetic generations across simulated time, a process that lacks a clear real-world analogue. **(ii) Computational limitations.** Full scale LLM model collapse experiments require iterative re-training and therefore remain extremely expensive, constraining empirical validation.

Our LWD framework is designed to bridge these gaps. We describe our experimental design in Section 3, and present empirical results in Section 4, showing that the norm of the embedded distance matrix decreases during collapse in both LLM and GMM experiments. The limiting behavior of the GMM setup is proved in Appendix A. In Sections 5 and 6, we discuss our findings and outline directions for future work.

3 Methods and Experiments

3.1 Experiment: Synthetic Conversations on the Internet

In our LLM Web Dynamics (LWD) framework, n different LLM models discuss a certain topic and get updated by answers from other participants over time. Full fine-tuning at each time is infeasible and expensive, so each model instead refreshes its context via retrieval-augmented generation (RAG). RAG is lightweight to deploy and has been proven

repeatedly showing equal or better performance in particular tasks comparing to fine-tuning in empirical studies (Balaguer et al., 2024; Cheng et al., 2025; Singh et al., 2025; Gupta et al., 2024), making it a practical and low-cost surrogate for iterative learning and training within the framework of LWD.

Suppose we have n LLMs $\{\mathcal{M}_i\}_{i=1}^n$, each pre-trained on different data. For instance, GPT-3.5 is trained largely on English-dominant data (Brown et al., 2020), whereas DeepSeek-67B draws from a bilingual data of Chinese content (DeepSeek-AI et al., 2024). These geographic and linguistic differences give the models heterogeneous priors over vocabulary, style, and factual knowledge, which is essential for studying cross-model information propagation (AlKhamissi et al., 2024; Gupta et al., 2025). To measure model performance, we use a fixed query q and define a set of sentences containing information related to this query q . Intuitively, this set functions as the Internet from which language models grab information. Hence, at each time $t = 1, 2, \dots$, each model augments itself by retrieving k_t sentences from this set to generate a response to the query. Here we allow each model to grab a different number of sentences (and hence different amounts of information) as t grows. In the standard RAG approach (Gao et al., 2024), LLM should retrieve the top k_t relevant sentences; in our case, the sentences in the set are all relevant to q by construction, so we draw k_t sentences uniformly at random from this set each time.

We denote this set of sentences at time t as $A^{(t)}$. If this set changes over time, each model’s response would change accordingly, and thus we denote the response of model $i \in \{1, \dots, n\}$ at time t to query q as $F_i^{(t)}(q)$. For a fixed query q , there is still randomness in an LLM’s output, so $F_i^{(t)}(q)$ is a random variable whose distribution depends on the model at time t and the query. Our goal is to measure model performance, so at each t , we ask every model L iterations to get L responses $(f_i^{(t)}(q))_1, \dots, (f_i^{(t)}(q))_L$ drawn independently from the distribution of $F_i^{(t)}(q)$.

At each time t , after all n models each generate L responses, we take one response from each model and “post” them to the “Internet” $A^{(t)}$. Under the i.i.d. assumption that we made previously, randomly picking one of L responses is probabilistically equivalent to simply taking the first one.

Thus, we can define the set A at $t + 1$ as:

$$A^{(t+1)} = A^{(t)} \cup \{(f_1^{(t)}(q))_1, \dots, (f_n^{(t)}(q))_1\}.$$

Hence $|A^{(t+1)}| = |A^{(t)}| + n$, reflecting that the Internet is increasingly filled with synthetic answers. If we begin with $|A^{(0)}|$ human-generated sentences, then at time t , the probability of retrieving a synthetic sentence from $A^{(t)}$ is $\frac{nt}{|A^{(0)}| + nt}$ (since we choose to retrieve them uniformly at random), which increasingly approaches 1 as t increases. Recall that at each t , each model fetches k_t sentences from $A^{(t)}$. We want to use this experiment to discuss the case when LLMs get trained and updated by the information on the Internet, so it is reasonable to make k_t proportional to $|A^{(t)}|$, i.e., $k_t = \lfloor \beta \cdot |A^{(t)}| \rfloor$ for a fixed hyperparameter β .

Using this procedure (illustrated in Figure 1), we can observe how model responses evolve over time. To analyze the responses statistically, we use the open source embedding model *nomic-embed-v1.5* (Nussbaum et al., 2024), denoted as ϕ , which maps each text $(f_i^{(t)}(q))_l$ to a numeric vector $(\phi \circ f_i^{(t)}(q))_l \in \mathbb{R}^{768}$, $l = 1, \dots, L$. This function ϕ allows us to quantify the similarity between two texts such that a smaller distance between embedding vectors indicates that the original two sentences are more semantically similar. Given these L vectors for each model i at time t , we can estimate the distribution of $(\phi \circ F_i^{(t)}(q))$. This can be challenging due to the high dimension of the embedding model, and one can adopt the framework of *Data-Kernel Perspective Space* (DKPS) (Helm et al., 2024), which reduces its dimension by Classical Multidimensional Scaling to get nice vector representations.

In addition to observing how the distribution evolves, we focus on estimating the distribution mean by averaging these L vectors to measure how model i responds to query q at time t :

$$X_i^{(t)} := \frac{1}{L} \sum_{l=1}^L (\phi \circ f_i^{(t)}(q))_l \in \mathbb{R}^{768}. \quad (1)$$

We claim that as t increases, the distributions of $F_i^{(t)}(q)$ and $F_j^{(t)}(q)$ for $i \neq j$, $i, j = 1, \dots, n$, become more similar. We aim to show this by comparing $X_i^{(t)}$ and $X_j^{(t)}$. In detail, we capture the pairwise model difference through a $n \times n$ matrix $D^{(t)}$ whose entries are defined as

$$D_{ij}^{(t)} := \|X_i^{(t)} - X_j^{(t)}\|_2, \quad i, j = 1, \dots, n \quad (2)$$

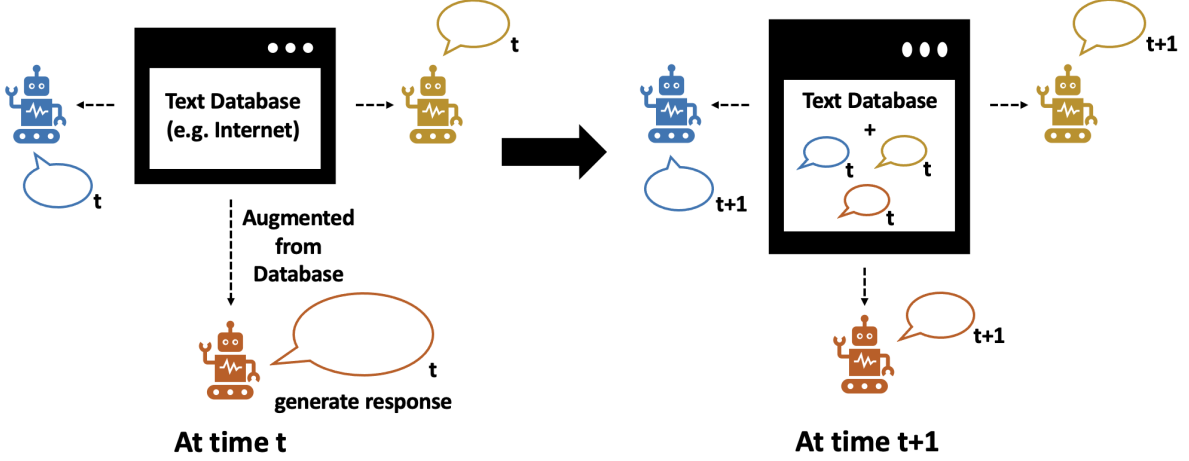


Figure 1: Experiment in Section 3.1, from t to $t + 1$. At time t , three different LLMs generate responses based on augmentation contexts fetched from a shared text database. They then post their responses to the text database, based on which they generate the next-time responses.

where $\|\cdot\|_2$ denotes the Euclidean norm. To discuss that model diversity shrinks under our experimental setting, we conjecture that

$$\left\|D^{(t)}\right\|_F \rightarrow c \text{ as } t \rightarrow \infty,$$

where $\|\cdot\|_F$ denotes the Frobenius norm, and c is a small nonnegative number that depends on some unknown intrinsic differences between models that are invariant to the environment. The detailed experiment is summarized in Algorithm 1, and we present examples in Section 4 to illustrate this conjecture.

3.2 A System of Gaussian Mixture Models

Next we design a system of Gaussian mixture models (GMMs) analogous to the mechanism in Section 3.1. Consider a collection of n time-varying GMMs in d -dimensional Euclidean space. For all models, we fix the number of components B , a single nondegenerate covariance matrix $\Sigma \in \mathbb{R}^{d \times d}$, and mean vectors $\mu_b \in \mathbb{R}^d$, $b = 1, \dots, B$. We define the i -th GMM at t , denoted as $g_i^{(t)}$, via the distribution

$$g_i^{(t)}(x) = \sum_{b=1}^B \pi_{i,b}^{(t)} \mathcal{N}(x; \mu_b, \Sigma), \quad (3)$$

where $\mathcal{N}(x; \mu_b, \Sigma)$ denotes the density of a normal distribution at x with parameters (μ_b, Σ) , and $\pi_{i,b}^{(t)}$ denotes the GMM's mixture weight at component b ; we collect the B mixture weights as the probability vector $\Pi_i^{(t)}$. We initialize each GMM with

different vectors $\Pi_i^{(t=0)}$. For example, one can sample each vector $\Pi_i^{(0)}$ from a Dirichlet distribution with parameter (a, \dots, a) .

Recall that $\phi \circ (F_i^{(t)}(q))$ denotes the i -th LLM model at time t , evaluated by query q and embedded by model ϕ . It follows some distribution, which can be approximated by certain GMM like $g_i^{(t)}$. The parameters in $g_i^{(t)}$, including $\{B, \Sigma, \mu_b, \Pi_i^{(t)}\}$, can be all time-varying; for simplicity, we fix most of them and only allow $\Pi_i^{(t)}$ to update at each time. Hence, GMM i at time t is characterized by its mixture weights, the pairwise distance between $g_i^{(t)}$ and $g_j^{(t)}$ is reduced to the distance between $\Pi_i^{(t)}$ and $\Pi_j^{(t)}$, and we can define the $n \times n$ distance matrix at time t as $D^{(t)}$:

$$(D^{(t)})_{ij} := \left\| \Pi_i^{(t)} - \Pi_j^{(t)} \right\|_2. \quad (4)$$

We then define a set of points A , similar to the set of texts ("the Internet") in Section 3.1. Let $A^{(0)}$ be the initialization of this set. At each t , each GMM $g_i^{(t)}$ generates L points: $s_{i,1}^{(t)}, \dots, s_{i,L}^{(t)}$ to be added to the set A :

$$A^{(t+1)} = A^{(t)} \cup \bigcup_{i=1}^n \{s_{i,1}^{(t)}, \dots, s_{i,L}^{(t)}\}.$$

This set is used to update each GMM in the following way: each model i randomly draws k_t points from $A^{(t)}$. As in Section 3.1, we put $k_t = \lfloor \beta \cdot |A^{(t)}| \rfloor$. Using $\Pi_i^{(t)}$ as the prior probabilities and these k_t points as observed data, we compute a posterior update of $\Pi_i^{(t+1)}$ via a revised update

Algorithm 1 Experiment: synthetic conversations on the Internet

Require: n different LLMs, nomic-embed-v1.5, a set of texts $A^{(0)}$, a fixed query q , a fixed L , a fixed β , total time T .

```
1: for timestep  $t = 0$  to  $T$  do
2:   for each model  $i = 1$  to  $n$  do
3:     Retrieve  $k_t$  sentences uniformly from  $A^{(t)}$ , where  $k_t := \lfloor \beta \cdot |A^{(t)}| \rfloor$ .
4:     Generate answers based on the retrievals  $L$  times:  $(f_i^{(t)}(q))_1, \dots, (f_i^{(t)}(q))_L$ .
5:     Embed them:  $(\phi \circ (f_i^{(t)}(q)))_1, \dots, (\phi \circ (f_i^{(t)}(q)))_L$  using nomic-embed-v1.5.
6:     Compute  $X_i^{(t)}$  using Eq.(1).
7:   end for
8:   Construct matrix  $D^{(t)}$  using Eq.(2). Compute  $\|D^{(t)}\|_F$ .
9:   Update the set  $A$ :  $A^{(t+1)} = A^{(t)} \cup \{(f_1^{(t)}(q))_1, \dots, (f_n^{(t)}(q))_1\}$ .
10:  Get  $F_i^{(t+1)}(q)$  corresponding to the updated  $A^{(t+1)}$ ,  $i = 1, \dots, n$ .
11: end for
```

algorithm in (Zivkovic and van der Heijden, 2004), as summarized in Algorithm 2:

Algorithm 2 Mixture-weight update algorithm

Require: Weight vector $\Pi_i^{(t)} = (\pi_{i,1}^{(t)}, \dots, \pi_{i,B}^{(t)})$, k_t points $\{u_1, \dots, u_{k_t}\}$, series of coefficients $\alpha_t \in (0, 1)$ and $c_{t,B}$, threshold $\epsilon \in [0, 1]$.

```
1: Initialize  $\pi_{i,b}^{(t+1)} \leftarrow \pi_{i,b}^{(t)}$  for all  $b = 1, \dots, B$ .
2: for  $u$  in  $\{u_1, \dots, u_{k_t}\}$  do
3:   Compute the ownership  $o_b = \pi_{i,b}^{(t+1)} \mathcal{N}(u; \mu_b, \Sigma) / g_i^{(t+1)}(u)$ ,  $b = 1, \dots, B$ ;  $g_i^{(t+1)}$  defined in Eq.(3).
4:   for  $b = 1$  to  $B$  do
5:      $\pi_{i,b}^{(t+1)} \leftarrow (1 - \alpha_t) \pi_{i,b}^{(t+1)} + \alpha_t \frac{o_b - c_{t,B}}{1 - B \cdot c_{t,B}}$ .
6:   end for
7:   for  $b = 1$  to  $B$  do
8:     if  $\pi_{i,b}^{(t+1)} \leq 0$  then
9:       for  $b' \neq b$  do
10:         $\pi_{i,b'}^{(t+1)} \leftarrow \frac{\pi_{i,b'}^{(t+1)}}{1 + \epsilon - \pi_{i,b}^{(t+1)}}$ .
11:      end for
12:       $\pi_{i,b}^{(t+1)} \leftarrow \epsilon$ .
13:    end if
14:  end for
15: end for
```

The update of $\Pi_i^{(t)}$ thus updates $g_i^{(t)}$ to $g_i^{(t+1)}$. This experiment is summarized in Algorithm 3. For this system of GMMs, we conjecture that:

$$\|D^{(t)}\|_F \rightarrow 0 \text{ as } t \rightarrow \infty, \quad (5)$$

i.e., that each pairwise distance $\|\Pi_i^{(t)} - \Pi_j^{(t)}\|_2$ converges to 0. Section 4 presents simulation results

to demonstrate this conjecture. We later prove this claim in Appendix A.

4 Results

4.1 LLM Experiment

To implement the experiment designed in Section 3.1, we try $n = 3$ models: Meta’s Llama-3.1-8B-Instruct (Dubey et al., 2024), DeepSeek’s deepseek-llm-7b-chat (Wang et al., 2023), and Mistral’s Mistral-7B-Instruct-v0.3 (Jiang et al., 2023). These three AI companies are headquartered in the U.S., China, and France respectively; we choose them so that the three models are pre-trained differently at least due to the distinct emphasis on contexts in their own languages. At $t = 0$, we construct the “Internet” $A^{(0)}$ by putting 20 posts about cryptocurrencies, collected and organized by (Ebrahimi, 2024): 7 are positive, 7 are neutral, and 6 are negative. The query we use is “Please provide EXACTLY one concise sentence about the future prospects of Bitcoin.”, and each model answers the question after reading posts sampled from $A^{(t)}$. We instruct them to answer exactly in one sentence because we want to focus on the semantic similarity or difference between these three models over time, instead of the language structure and complexity difference. The latter is also interesting to explore, but requires other statistical tools on texts, such as the depth of parse tree of sentences. We aim to investigate this in our future work.

We then follow Algorithm 1 to simulate the experiment for $T = 60$. We set $L = 40$ and $\beta = 0.5$.

Algorithm 3 Simulation of a GMM system

Require: Number of models n , dimension d , number of components B , covariance matrix Σ , mean vectors $\{\mu_b\}_{b=1}^B$, positive integer L , fixed coefficient β , total time T .

```

1: Initialize mixture coefficients  $\Pi_i^{(t)} \sim \text{Dir}(a)$  and  $A^{(0)}$ .
2: for timestep  $t = 0$  to  $T$  do
3:   Construct matrix  $D^{(t)}$  using Eq.(4). Compute  $\|D^{(t)}\|_F$ .
4:   for each model  $i = 1$  to  $n$  do
5:     Generate  $L$  points  $s_{i,1}^{(t)}, \dots, s_{i,L}^{(t)}$ .
6:     Sample  $k_t := \lfloor \beta \cdot |A^{(t)}| \rfloor$  points uniformly from  $A^{(t)}$ , say,  $\{u_1^{(t)}, u_2^{(t)}, \dots, u_{k_t}^{(t)}\}$ .
7:     Update  $\Pi_i^{(t)}$  to  $\Pi_i^{(t+1)}$  via Algorithm 2 using data  $\{u_1^{(t)}, u_2^{(t)}, \dots, u_{k_t}^{(t)}\}$ . This also updates the
       GMM from  $g_i^{(t)}$  to  $g_i^{(t+1)}$ .
8:   end for
9:   Update  $A$ :  $A^{(t+1)} = A^{(t)} \cup \bigcup_{i=1}^n \{s_{i,1}^{(t)}, \dots, s_{i,L}^{(t)}\}$ .
10: end for

```

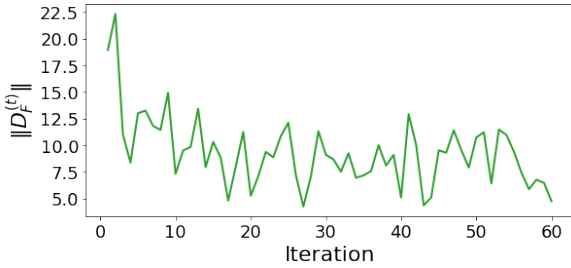


Figure 2: $\|D^{(t)}\|_F$ defined in Eq.(2) over time.

The experiment was conducted on Nvidia A100 80GB GPUs, AMD EPYC 7443 24 Core, taking approximately 8 hours to complete the full process. Figure 2 shows that the norm decreases from over 20 to around 5, indicating that the average responses generated by these three models are becoming more similar semantically.

In fact, this phenomenon is obvious when we directly compare the posts generated by three models at first and at $T = 60$:

- At $t = 1$, Llama: *Bitcoin's price is expected to remain stable around \$30,000 as the market awaits the Federal Reserve's announcement on interest rates despite recent fluctuations in global hash rate and market volatility.*
- At $t = 1$, deepseek: *Bitcoin's future prospects are expected to continue gaining mainstream adoption, with major institutions like PayPal, JPMorgan, and Tesla integrating crypto into their services and products.*
- At $t = 1$, Mistral: *The future prospects of Bitcoin continue to evolve, with increasing*

institutional adoption, regulatory decisions, and the emergence of new stablecoins and CBDCs impacting its growth potential.

- At $t = 60$, Llama: *The future prospects of Bitcoin are marked by growing mainstream adoption, institutional integration, increased user base, and regulatory decisions, while facing market volatility and security concerns.*
- At $t = 60$, deepseek: *The future prospects of Bitcoin indicate continued mainstream adoption, influenced by increasing institutional integration, a growing user base, and regulatory decisions, while facing market volatility and security concerns.*
- At $t = 60$, Mistral: *The future prospects of Bitcoin suggest continued mainstream adoption, driven by increasing institutional integration, a growing user base, and regulatory decisions, while facing market volatility and security concerns.*

We can see that the three models initially provide opinions from different perspectives, but eventually, they become almost identical semantically.

Recall that at each time t , we generate $L = 40$ responses for each model so that we can examine their distributions. Since each embedded response is a vector of length 768, we perform Classical Multidimensional Scaling on the pairwise distance matrix so that we can plot each response in a 2-D space. From Figure 3, we can see that at the beginning, the distributions of three models' responses look very different, but at T , they are all point

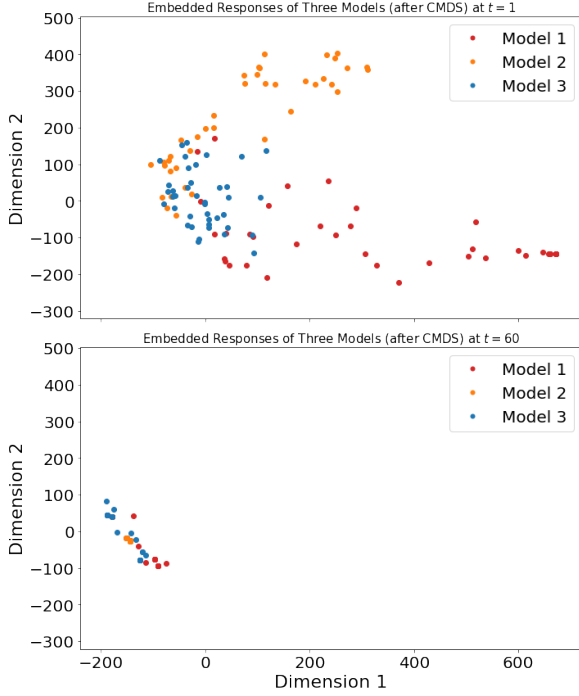


Figure 3: Scatter plots of three models' responses at $t = 1$ and $t = T$.

masses that are close to each other. This indicates that the three models are not only less diverse from each other, but also exhibit reduced internal diversity within themselves in the simulated Internet environment populated with synthetic posts.

4.2 GMM Experiment

Next we present some results of our GMM experiment described in Section 3.2 to demonstrate how it's phenomenally similar to the LLM experiment. First, we define three two-component GMMs ($B = 2$). The component means are $\mu_1 = -5$, $\mu_2 = 5$, and the variances are both $\Sigma_1 = \Sigma_2 = 1$. The initial weights are sampled from Dirichlet with $a = 1$, and same as the LLM experiment, we set $\beta = 0.5$. As suggested by Zivkovic and van der Heijden (2004), we set $\alpha_t = k_t^{-1}$; since $B \cdot c_{t,B}$ should be smaller than 1, we take $c_{t,B} = 1/(k_t \cdot B^2)$. We take $L = 3$ and $T = 200$.

Figure 4 shows how $\|D^{(t)}\|_F$ evolves in 5 replicates (i.e. by running the simulation 5 times with different seeds) - they all seem to converge to 0.

Since GMM has an analytical form of density, we plot histograms of our three GMMs at different times. From Figure 5, we can see that they start with very different component weights but seem to converge to a same weight vector.

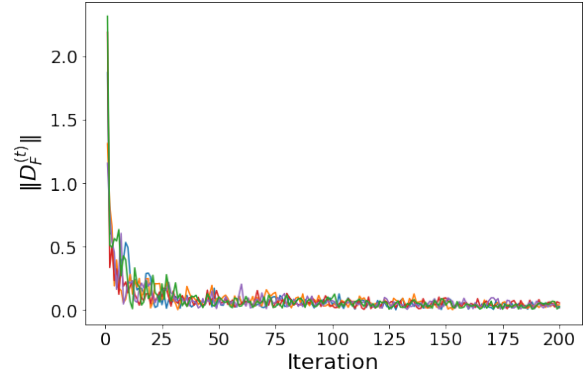


Figure 4: $\|D^{(t)}\|_F$ defined in Eq. (4) over time.

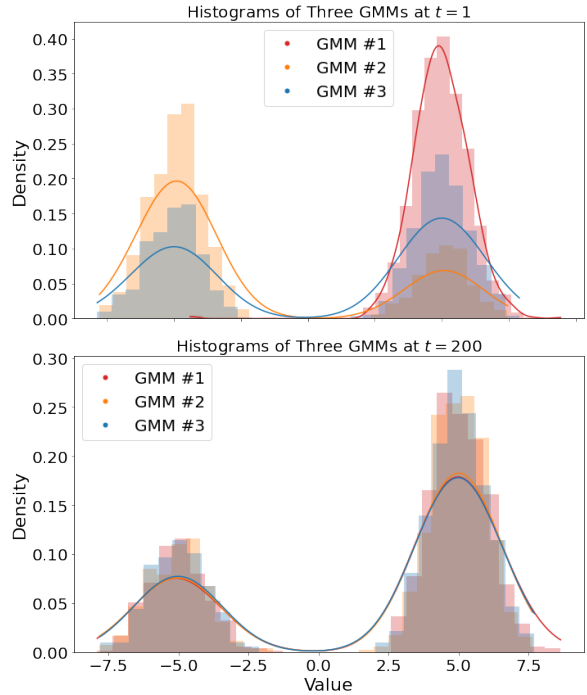


Figure 5: Histograms of three GMMs $t = 1$ and $t = T$.

Indeed, we can formulate our claim (5) as: for $i, j \in \{1, \dots, n\}$,

$$\Pi_i^{(t)} - \Pi_j^{(t)} \rightarrow 0 \text{ as } t \rightarrow \infty. \quad (6)$$

We prove this claim in expectation, and we present the sketch of the proof in Appendix A.

When comparing the simulation results of our LLM and GMM experiments, we observe similar phenomena. Prior work, such as Shumailov et al. (2024), has also drawn parallels between LLM experiments and GMM setups. As a result, establishing theoretical claims in the GMM setting offers theoretical support for the behaviors observed in our LLM experiments.

However, we observe that the pattern of diminishing norms in Figure 4 looks smoother than

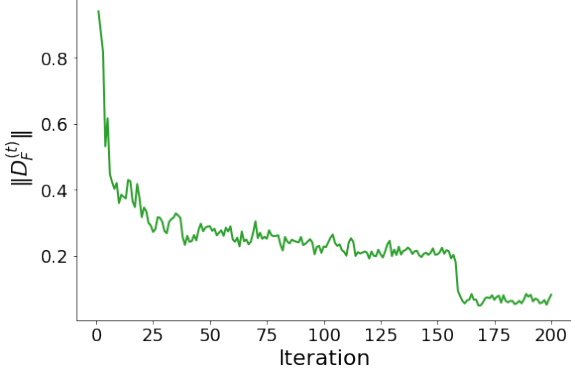


Figure 6: $\|D^{(t)}\|_F$ defined in Eq. (4) over time.

that of LLMs in Figure 2. This is because two-component GMM is much simpler than LLM. Using GMMs with a larger number of components serves as a better proxy for LLMs, as the additional components offer greater capacity to capture complex distributions.

Figure 6 gives an example of our experiment using three GMMs of $B = 11$ components. $\|D^{(t)}\|_F$ also seems to converge to 0, but the line looks less smooth and closer to the LLM plot. Interestingly, we see a sudden fall of $\|D^{(t)}\|_F$ around $t = 160$ in Figure 6. Therefore, it is highly likely that in our LLM experiment, the norm of the distance matrix between models will continue to decrease at some larger t . This highlights another advantage of our GMM setup—it serves as a useful proxy by offering insights into potential behaviors in the LLM experiment.

5 Discussion

Our experiments demonstrate that model collapse can be observed and quantified in a fully API-accessible LLM network with RAG engine that mimics real-world Internet usage. By embedding individual responses and tracking the variation in induced Frobenius norm of the pairwise distance matrix, we observe a norm decay toward a small value, indicating that all agents have converged to an information neutral equilibrium. Importantly, this convergence should not be viewed as intrinsically *good* or *bad*; it merely signifies that further training using synthetic data shall no longer alter communication dynamics. Essentially the network used up all the information entropy from the raw data and communication built on the network is stabilized. Whether such “neutral” collapse is detrimental depends on goals of downstream tasks.

Our GMM setup within the LWD framework ex-

hibits limiting behavior that closely mirrors that of our LLM experiment. One minor difference is the limiting value: we prove that the distance matrix norm in the GMM setting converges to zero in expectation, whereas in the LLM network, we only conjecture convergence to a small, non-negative value. The discrepancy arises because a B -component GMM is restricted to a finite parametrization, while a Transformer-based LLM occupies an effectively infinite-dimensional function space (Pérez et al., 2019; Yang, 2020).

This distinction underscores a key advantage of our GMM proxy: its extensibility via changing parameterization. As demonstrated in Section 4, GMMs with more components produce convergence patterns that more similar to those observed in real LLMs, illustrating the framework’s improved fidelity over simpler statistical surrogates. Moreover, in our setup, the means and variances of the Gaussians are fixed, and only the mixture weights are updated. These parameters can also be made time-varying, providing additional flexibility in approximating LLM dynamics. Importantly, simulating interactions in such complicated GMM system requires only minutes of computation, offering a highly efficient alternative for studying synthetic data pipelines before committing to expensive LLM experiments.

6 Limitations

Despite the promise of our LLM Web Dynamics, several limitations remain. Our current study focuses on *pattern learning* where we characterize collapse by geometric drift in terms of the diminishing norm of pairwise distance matrix in the embedded vector space. Because LLMs and their interaction graphs are essentially black-box models, these results could also be better justified by *further statistical inference*. Therefore a key next step is to transform the pattern learning into systematic hypothesis testing or inference framework, providing finite-sample, high-probability guarantees. Finally, the LWD with RAG engine serves as a controllable testbed to quantify, isolate and examine the effect of different variables during the process of model collapse. Covariate like synthetic-to-real ratio, the distribution and quality of real data, and possible irrelevant noisy data perturbation can be incorporated into the framework LWD and produce predictable model collapse for various downstream tasks.

Acknowledgments

This work was supported by Air Force Office of Scientific Research (AFOSR) Complex Networks award number FA9550-25-1-0128, and Defense Advanced Research Projects Agency (DARPA) Artificial Intelligence Quantified award number HR00112520026.

References

- Sina Alemohammad, Josue Casco-Rodriguez, Lorenzo Luzi, Ahmed Imtiaz Humayun, Hossein Babaei, Daniel LeJeune, Ali Siahkoobi, and Richard G. Baraniuk. 2023. [Self-consuming generative models go mad](#). *Preprint*, arXiv:2307.01850.
- Badr AlKhamissi, Muhammad ElNokrashy, Mai AlKhamissi, and Mona Diab. 2024. [Investigating cultural alignment of large language models](#). *Preprint*, arXiv:2402.13231.
- Angels Balaguer, Vinamra Benara, Renato Luiz de Freitas Cunha, Roberto de M. Estevão Filho, Todd Hendry, Daniel Holstein, Jennifer Marsman, Nick Mecklenburg, Sara Malvar, Leonardo O. Nunes, Rafael Padilha, Morris Sharp, Bruno Silva, Swati Sharma, Vijay Aski, and Ranveer Chandra. 2024. [Rag vs fine-tuning: Pipelines, tradeoffs, and a case study on agriculture](#). *Preprint*, arXiv:2401.08406.
- Quentin Bertrand, Avishek Joey Bose, Alexandre Duplessis, Marco Jiralerspong, and Gauthier Gidel. 2024. [On the stability of iterative retraining of generative models on their own data](#). *Preprint*, arXiv:2310.00429.
- Matyas Bohacek and Hany Farid. 2025. [Nepotistically trained generative-ai models collapse](#). *Preprint*, arXiv:2311.12202.
- Ali Borji. 2024. [A note on shumailov et al. \(2024\): ‘ai models collapse when trained on recursively generated data’](#). *Preprint*, arXiv:2410.12954.
- Tom B. Brown, Benjamin Mann, Nick Ryder, Melanie Subbiah, Jared Kaplan, Prafulla Dhariwal, Arvind Neelakantan, Pranav Shyam, Girish Sastry, Amanda Askell, Sandhini Agarwal, Ariel Herbert-Voss, Gretchen Krueger, Tom Henighan, Rewon Child, Aditya Ramesh, Daniel M. Ziegler, Jeffrey Wu, Clemens Winter, and 12 others. 2020. [Language models are few-shot learners](#). *Preprint*, arXiv:2005.14165.
- Mingyue Cheng, Yucong Luo, Jie Ouyang, Qi Liu, Huijie Liu, Li Li, Shuo Yu, Bohou Zhang, Jiawei Cao, Jie Ma, Daoyu Wang, and Enhong Chen. 2025. [A survey on knowledge-oriented retrieval-augmented generation](#). *Preprint*, arXiv:2503.10677.
- DeepSeek-AI, :, Xiao Bi, Deli Chen, Guanting Chen, Shanhuang Chen, Damai Dai, Chengqi Deng, Honghui Ding, Kai Dong, Qiu Shi Du, Zhe Fu, Huazuo Gao, Kaige Gao, Wenjun Gao, Ruiqi Ge, Kang Guan, Daya Guo, Jianzhong Guo, and 69 others. 2024. [Deepseek llm: Scaling open-source language models with longtermism](#). *Preprint*, arXiv:2401.02954.
- Apratim Dey and David Donoho. 2024. [Universal-ity of the \$\pi^2/6\$ pathway in avoiding model collapse](#). *Preprint*, arXiv:2410.22812.
- Elvis Dohmatob, Yunzhen Feng, Arjun Subramonian, and Julia Kempe. 2024. [Strong model collapse](#). *Preprint*, arXiv:2410.04840.
- Abhimanyu Dubey, Abhinav Jauhri, Abhinav Pandey, Abhishek Kadian, Ahmad Al-Dahle, Aiesha Letman, Akhil Mathur, Alan Schelten, Amy Yang, Angela Fan, and 1 others. 2024. The llama 3 herd of models. *arXiv preprint arXiv:2407.21783*.
- Pejman Ebrahimi. 2024. [Crypto semantic news](#).
- Yunfan Gao, Yun Xiong, Xinyu Gao, Kangxiang Jia, Jinliu Pan, Yuxi Bi, Yi Dai, Jiawei Sun, Meng Wang, and Haofen Wang. 2024. [Retrieval-augmented generation for large language models: A survey](#). *Preprint*, arXiv:2312.10997.
- Matthias Gerstgrasser, Rylan Schaeffer, Apratim Dey, Rafael Rafailov, Henry Sleight, John Hughes, Tomasz Korbak, Rajashree Agrawal, Dhruv Pai, Andrey Gromov, Daniel A. Roberts, Diyi Yang, David L. Donoho, and Sanmi Koyejo. 2024. [Is model collapse inevitable? breaking the curse of recursion by accumulating real and synthetic data](#). *Preprint*, arXiv:2404.01413.
- Nate Gillman, Michael Freeman, Daksh Aggarwal, Chia-Hong Hsu, Calvin Luo, Yonglong Tian, and Chen Sun. 2024. [Self-correcting self-consuming loops for generative model training](#). *Preprint*, arXiv:2402.07087.
- Ian Goodfellow, Yoshua Bengio, and Aaron Courville. 2016. *Deep Learning*. MIT Press. <http://www.deeplearningbook.org>.
- Shailja Gupta, Rajesh Ranjan, and Surya Narayan Singh. 2024. [A comprehensive survey of retrieval-augmented generation \(rag\): Evolution, current landscape and future directions](#). *Preprint*, arXiv:2410.12837.
- Vansh Gupta, Sankalan Pal Chowdhury, Vilém Zouhar, Donya Rooein, and Mrinmaya Sachan. 2025. [Multilingual performance biases of large language models in education](#). *Preprint*, arXiv:2504.17720.
- Hengzhi He, Shirong Xu, and Guang Cheng. 2025. [Golden ratio weighting prevents model collapse](#). *Preprint*, arXiv:2502.18049.
- Hayden Helm, Brandon Duderstadt, Youngser Park, and Carey Priebe. 2024. [Tracking the perspectives of interacting language models](#). In *Proceedings of*

- the 2024 Conference on Empirical Methods in Natural Language Processing, pages 1508–1519, Miami, Florida, USA. Association for Computational Linguistics.
- Albert Q. Jiang, Alexandre Sablayrolles, Arthur Mensch, Chris Bamford, Devendra Singh Chaplot, Diego de las Casas, Florian Bressand, Gianna Lengyel, Guillaume Lample, Lucile Saulnier, L  lio Renard Lavaud, Marie-Anne Lachaux, Pierre Stock, Teven Le Scao, Thibaut Lavril, Thomas Wang, Timoth  e Lacroix, and William El Sayed. 2023. [Mistral 7b](#). *Preprint*, arXiv:2310.06825.
- Jared Kaplan, Sam McCandlish, Tom Henighan, Tom B. Brown, Benjamin Chess, Rewon Child, Scott Gray, Alec Radford, Jeffrey Wu, and Dario Amodei. 2020. [Scaling laws for neural language models](#). *Preprint*, arXiv:2001.08361.
- Joshua Kazdan, Rylan Schaeffer, Apratim Dey, Matthias Gerstgrasser, Rafael Rafailov, David L. Donoho, and Sanmi Koyejo. 2025. [Collapse or thrive? perils and promises of synthetic data in a self-generating world](#). *Preprint*, arXiv:2410.16713.
- Ying Li, Zhidi Lin, Feng Yin, and Michael Minyi Zhang. 2024. [Preventing model collapse in gaussian process latent variable models](#). *Preprint*, arXiv:2404.01697.
- Keith Man and Javaan Chahl. 2022. [A review of synthetic image data and its use in computer vision](#). *Journal of Imaging*, 8(11).
- Gonzalo Mart  nez, Lauren Watson, Pedro Reviriego, Jos   Alberto Hern  ndez, Marc Juarez, and Rik Sarkar. 2023. [Combining generative artificial intelligence \(ai\) and the internet: Heading towards evolution or degradation?](#) *Preprint*, arXiv:2303.01255.
- Zach Nussbaum, John X. Morris, Brandon Duderstadt, and Andriy Mulyar. 2024. [Nomic embed: Training a reproducible long context text embedder](#). *Preprint*, arXiv:2402.01613.
- Jorge P  rez, Javier Marinkovi  , and Pablo Barcel  . 2019. [On the turing completeness of modern neural network architectures](#). *Preprint*, arXiv:1901.03429.
- Rylan Schaeffer, Joshua Kazdan, Alvan Caleb Arulandu, and Sanmi Koyejo. 2025. [Position: Model collapse does not mean what you think](#). *Preprint*, arXiv:2503.03150.
- Mohamed El Amine Seddik, Suei-Wen Chen, Soufiane Hayou, Pierre Youssef, and Merouane Debbah. 2024. [How bad is training on synthetic data? a statistical analysis of language model collapse](#). *Preprint*, arXiv:2404.05090.
- Ilia Shumailov, Zakhar Shumaylov, Yiren Zhao, Yarin Gal, Nicolas Papernot, and Ross Anderson. 2024. [The curse of recursion: Training on generated data makes models forget](#). *Preprint*, arXiv:2305.17493.
- Aditi Singh, Abul Ehtesham, Saket Kumar, and Tala Talei Khoei. 2025. [Agentic retrieval-augmented generation: A survey on agentic rag](#). *Preprint*, arXiv:2501.09136.
- Ananda Theertha Suresh, Andrew Thangaraj, and Aditya Nanda Kishore Khandavally. 2024. [Rate of model collapse in recursive training](#). *Preprint*, arXiv:2412.17646.
- Pablo Villalobos, Anson Ho, Jaime Sevilla, Tamay Besiroglu, Lennart Heim, and Marius Hobbhahn. 2024. [Will we run out of data? limits of llm scaling based on human-generated data](#). *Preprint*, arXiv:2211.04325.
- Guan Wang, Sijie Cheng, Xianyuan Zhan, Xiangang Li, Sen Song, and Yang Liu. 2023. Openchat: Advancing open-source language models with mixed-quality data. *arXiv preprint arXiv:2309.11235*.
- Sierra Wyllie, Ilia Shumailov, and Nicolas Papernot. 2024. [Fairness feedback loops: Training on synthetic data amplifies bias](#). *Preprint*, arXiv:2403.07857.
- Greg Yang. 2020. [Tensor programs ii: Neural tangent kernel for any architecture](#). *Preprint*, arXiv:2006.14548.
- Zoran Zivkovic and Ferdinand van der Heijden. 2004. Recursive unsupervised learning of finite mixture models. *IEEE Transactions on pattern analysis and machine intelligence*, 26(5):651–656.

A Sketch of Proof for GMM Experiment

In this section, we discuss our conjecture (5) mathematically. In the GMM experiment, we measure the GMMs’ weight differences in the distance matrix, so the matrix norm converging to 0 is equivalent to pairwise weight differences going to 0.

For now, suppose we do not do the positive normalization step in Algorithm 2. Let us consider the update of GMM $i = 1, \dots, N$ with points $u_1^{(t)}, \dots, u_{k_t}^{(t)}$ sampled uniformly at random without replacement from $A^{(t)}$ (we denote this distribution as $\mathcal{U}(A^{(t)})$). Let us also consider the update for just one $u_j^{(t)}$ (i.e., one iteration of the outer for-loop in Algorithm 2). The mixture-weight update for component $b = 1, \dots, B$ is then

$$\pi_{i,b}^{(t+1)} \leftarrow (1 - \alpha_t) \pi_{i,b}^{(t)} + \frac{\alpha_t}{1 - B c_{t,B}} \left\{ o_{i,b}^{(t)}(u_j^{(t)}) - c_B \right\}. \quad (7)$$

Let us integrate the RHS over $u_j^{(t)} \sim \mathcal{U}(A^{(t)})$ for some arbitrary $j \in \{1, \dots, k_t\}$. For mathematical simplicity, suppose $A^{(0)}$ is empty. Under this simplifying assumption, the set $A^{(t)}$ contains only points generated from a (possibly previous)

GMM, so the update point $u_j^{(t)}$ must have been generated by some GMM in an earlier step. Because the k_t update points $u_1^{(t)}, u_2^{(t)}, \dots, u_{k_t}^{(t)}$ are drawn simultaneously from the same distribution, the order in which an update point is drawn does not affect the probability of which GMM (among $\{(i', t') : i' \in [n], t' \in [t-1]\}$) the point is drawn from. Hence, we can say that $u_j^{(t)}$ is drawn from GMM $g_{i'}^{(t')}$ with probability $p_{i'}^{(t')} = (nt)^{-1}$. We then integrate the ownership $o_{i,b}^{(t)}(u_j^{(t)})$, which is the only term in the RHS of (7) that involves the update point:

$$\int o_{i,b}^{(t)}(u) dg_{i'}^{(t')}(u) \equiv \int \frac{\pi_{i,b}^{(t)} N(u; \mu_b, \Sigma)}{g_i^{(t)}(u)} dg_{i'}^{(t')}(u) \quad (8)$$

$$= \pi_{i,b}^{(t)} \int \frac{g_{i'}^{(t')}(u)}{g_i^{(t)}(u)} dN(u; \mu_b, \Sigma) \quad (9)$$

where $g_i^{(t)}(u) = \sum_{\ell=1}^B \pi_{i,\ell}^{(t)} N(u; \mu_\ell, \Sigma)$ is the likelihood of GMM i at u . Because the GMM component parameters are fixed (only the mixture weights vary), if the mixture variances are small enough (almost same as saying if the mixture components are well-separated enough), then we can make the approximation $\frac{g_{i'}^{(t')}(u)}{g_i^{(t)}(u)} \approx \sum_{\ell=1}^B \frac{\pi_{i',\ell}^{(t')}}{\pi_{i,\ell}^{(t)}} 1_{(u=\mu_\ell)}$. We also have that $N(u; \mu_b, \Sigma)$ is almost zero if u is far enough away from μ_b , so we can approximate

$$\int \frac{g_{i'}^{(t')}(u)}{g_i^{(t)}(u)} N(u; \mu_b, \Sigma) du \approx \frac{\pi_{i',b}^{(t')}}{\pi_{i,b}^{(t)}}$$

so then Eq.(8) is approximated as $\pi_{i',b}^{(t')}$. Under this assumption, the integral of the RHS of Eq.(7) over $u_j^{(t)} \sim \mathcal{U}(A^{(t)})$ is approximately

$$\approx (1 - \alpha_t) \pi_{i,b}^{(t)} + \alpha_t \frac{\bar{\pi}_b^{(t)} - c_{t,B}}{1 - Bc_{t,B}} \quad (10)$$

where we introduce the notation

$$\bar{\pi}_b^{(t)} := \sum_{i'=1}^n \sum_{t'=0}^{t-1} p_{i'}^{(t')} \pi_{i',b}^{(t')} = (nt)^{-1} \sum_{i'=1}^n \sum_{t'=0}^{t-1} \pi_{i',b}^{(t')},$$

which is component b 's mixture weight averaged over all n models and all past times $0, \dots, t-1$. If $0 < c_{t,B} < \min\{B^{-1}, \bar{\pi}_b^{(t)}\}$, then $\frac{\bar{\pi}_b^{(t)} - c_{t,B}}{1 - Bc_{t,B}}$ in (10) is positive, which guarantees that the entire term in (10) is also positive.

If we do this update for each of the k_t points, the ultimate update (in expectation) for $\pi_{i,b}^{(t+1)}$ is

$$\begin{aligned} &\approx \bar{\alpha}_t^{k_t} \pi_{i,b}^{(t)} + \alpha_t \frac{\bar{\pi}_b^{(t)} - c_{t,B}}{1 - Bc_{t,B}} \sum_{s=0}^{k_t-1} \bar{\alpha}_t^s \\ &= \bar{\alpha}_t^{k_t} \pi_{i,b}^{(t)} + \{1 - \bar{\alpha}_t^{k_t+1}\} \left[\frac{\bar{\pi}_b^{(t)} - c_{t,B}}{1 - Bc_{t,B}} \right] \end{aligned}$$

where we introduce the notation $\bar{\alpha}_t = 1 - \alpha_t$. Thus, at each t , the updated mixture-weight $\pi_{i,b}^{(t+1)}$ will, in expectation, be a convex combination of the (scaled) mixture weight $\pi_{i,b}^{(t)} / (1 - \alpha_t)$ and the value in the square brackets, which does not depend on which of the n GMMs is being updated. In particular, for any i and i' where $i \neq i'$, we have

$$\pi_{i,b}^{(t+1)} - \pi_{i',b}^{(t+1)} \leftarrow \approx (1 - \alpha_t)^{k_t} [\pi_{i,b}^{(t)} - \pi_{i',b}^{(t)}].$$

If $\alpha_t = k_t^{-1}$, which is suggested by [Zivkovic and van der Heijden \(2004\)](#), then because $\lim_{k_t \rightarrow \infty} (1 - \alpha_t)^{k_t} = e^{-1}$ is a nonnegative constant strictly smaller than 1 and $\lim_{t \rightarrow \infty} k_t = \infty$, we conclude that $\lim_{t \rightarrow \infty} |\pi_{i,b}^{(t)} - \pi_{i',b}^{(t)}| = 0$.